

VOLUME 38 NUMBER 2
FEBRUARY 2020

ISSN: 1002-0721
CODEN JREAE 6

Journal of
Rare Earths



CONTENTS

REVIEW

Luminescence thermal quenching of $M_2SiO_4:Eu^{2+}$ ($M=Sr, Ba$) phosphors.....*Shirun Yan* 113

SPECTROSCOPY, LUMINESCENCE AND PHOSPHORS

- X-ray-activated UVA long persistent luminescence from defective fluoride elpasolites
.....*Zhiyong Li, Hong Li, Hong-Tao Sun* 124
- Energy transfer and cross-relaxation induced multicolor upconversion emissions in $Er^{3+}/Tm^{3+}/Yb^{3+}$ doped double perovskite La_2ZnTiO_6 phosphors.....*Youfusheng Wu, Fengqin Lai, Bin Liu, Zhibiao Li, Tongxiang Liang, Yaochun Qiang, Jianhui Huang, Xinyu Ye, Weixiong You* 130
- Effect of chloride on spectrum properties of Pr^{3+}/Ho^{3+} co-doped fluorozirconate glasses
.....*Ya Zou, Yajie Wang, Shuai Han, Ying Du, Danping Chen, QiuHong Yang* 139
- Construction of NIR luminescent nanoscale lanthanide complexes with new flexible Schiff base ligands
.....*Bichen Yuan, Junbin Tao, Fei Wang, Chaoqun Zhu, Min Li, Xiaoping Yang* 143

RARE EARTH CATALYSIS

- Enhanced photocatalytic activities of Nd-doped TiO_2 under visible light using a facile sol-gel method
.....*Jicai Liang, Jingya Wang, Kexian Song, Xiaofeng Wang, Kaifeng Yu, Ce Liang* 148
- Effects of MO_x ($M=Mn, Cu, Sb, La$) on V–Mo–Ce/Ti selective catalytic reduction catalysts
.....*Daojun Zhang, Ziran Ma, Baodong Wang, Qi Sun, Wenqiang Xu, Tao Zhu* 157
- Enhancement of La_2O_3 to Li–Mn/ WO_3/TiO_2 for oxidative coupling of methane
.....*Fei Cheng, Jian Yang, Liang Yan, Jun Zhao, Huahua Zhao, Huanling Song, Ling Jun Chou* 167
- Ce–Fe–Mn ternary mixed-oxide catalysts for catalytic decomposition of ozone at ambient temperatures
.....*Xiao Chen, Zhenglong Zhao, Shuo Liu, Jinxing Huang, Jing Xie, Ying Zhou, Zhiyan Pan, Hanfeng Lu* 175

MAGNETISM AND MAGNETIC MATERIALS

- Zirconium content induced mitigation of mechanical anisotropy in 2:17 type SmCo magnets
.....*Guanghui Yan, Zhuang Liu, Yanping Feng, Weixing Xia, Chaoyue Zhang, Guangqing Wang, Aru Yan* 182
- Synthesis and characterization of $Co_{1-2x}Ni_xMn_xCe_yFe_{2-y}O_4$ nanoparticles
.....*Munirah Abdullah Almessiere, Yassine Slimani, Abdulhadi Baykal* 188

ADVANCED RARE EARTH MATERIALS

- Enhancing mechanical properties and air permeability of corundum porous materials by *in situ* formation of $LaAl_{11}O_{18}$ in bonding phase*Xin Xiong, Zhoufu Wang, Xitang Wang, Hao Liu, Yan Ma* 195

CHEMISTRY AND HYDROMETALLURGY

- Enhanced separation of praseodymium and neodymium by kinetic “push and pull” system of $[A336][NO_3]$ -DTPA in a column extractor*Xiaoqin Wang, Kun Huang, Wenjuan Cao, Pan Sun, Na Sui, Weiyuan Song, Huizhou Liu* 203

RARE EARTH APPLICATIONS

- Effect of Sr^{2+} and Dy^{3+} co-doping on coloration and temperature stabilization of a γ - Ce_2S_3 red pigment
.....*Yueming Li, Qi Liu, Fusheng Song, Zhumei Wang, Zongyang Shen, Yan Hong* 213

GEOLOGY AND ORE DRESSING

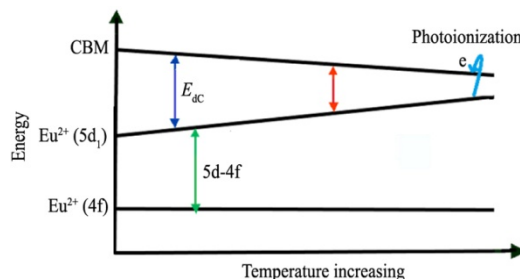
- Rare earth elements of fly ash from Wyoming's Powder River Basin coal
.....*Zaixing Huang, Maohong Fan, Hanjing Tian* 219

CONTENTS

REVIEW

- 113 Luminescence thermal quenching of $M_2SiO_4:Eu^{2+}$ (M=Sr, Ba) phosphors

Shirun Yan



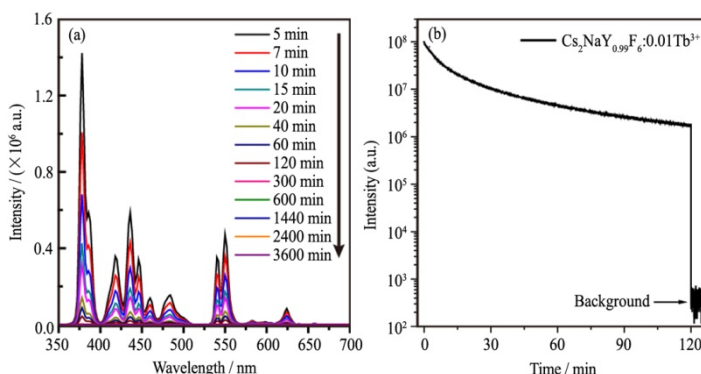
A less rigid lattice and hence a larger CTE of M_2SiO_4 host would result in a greater reduction in E_{ac} and as a consequence a more pronounced ionization of 5d electron of Eu^{2+} in $M_2SiO_4:Eu^{2+}$ at high temperatures

J. Rare Earths, (38) 2020: 113-123

SPECTROSCOPY, LUMINESCENCE AND PHOSPHORS

- 124 X-ray-activated UVA long persistent luminescence from defective fluoride elpasolites

Zhiyong Li, Hong Li, Hong-Tao Sun

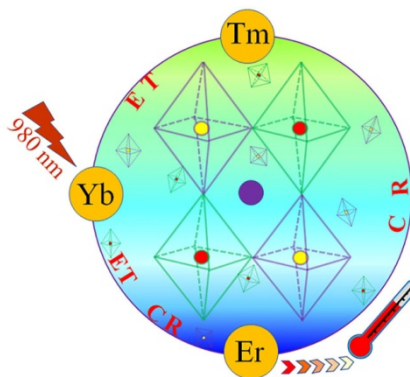


UVA afterglow of Tb^{3+} -doped fluoride elpasolite with a nominal composition of $Cs_2NaY_{0.99}F_6:0.01Tb^{3+}$ and with X-ray irradiation for 600 s. (a) Afterglow spectra recorded at different time after ceasing X-ray irradiation. The emission band peaking at 380 nm can be assigned to the transitions of $^5D_3 \rightarrow ^7F_6$. In addition to the UVA emissions, visible emission bands were also observed. (b) Afterglow decay detected at 380 nm as a function of time. The data were taken from 5 min after stopping the X-ray irradiation. The results show that $Cs_2NaY_{0.99}F_6:0.01Tb^{3+}$ sample exhibits the strongest afterglow luminescence intensity, and the duration can last more than 50 h after irradiation by X-ray source

J. Rare Earths, (38) 2020: 124-129

- 130 Energy transfer and cross-relaxation induced multicolor upconversion emissions in $Er^{3+}/Tm^{3+}/Yb^{3+}$ doped double perovskite La_2ZnTiO_6 phosphors

Youfusheng Wu, Fengqin Lai, Bin Liu, Zhibiao Li, Tongxiang Liang, Yaochun Qiang, Jianhui Huang, Xinyu Ye, Weixiong You

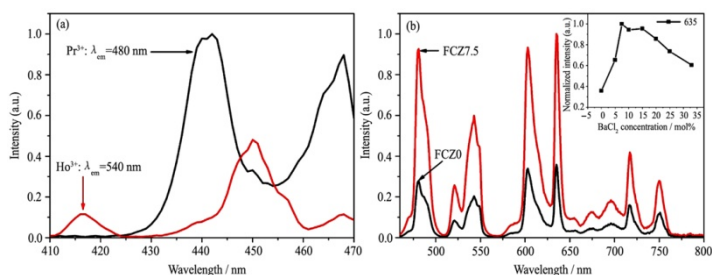


This graphic depicts all the elements including the LZT host with a double perovskite structure demonstrated by typical octahedrons, the dopants (Yb^{3+} , Er^{3+} and Tm^{3+}), mainly emitting colors with yellowish green, cyan and blue that are shown in gradually varying colors from the top (yellowish green) to middle (cyan) to bottom (blue), upconverting ET and CR processes and the outstretched potential application in temperature sensing

J. Rare Earths, (38) 2020: 130-138

- 139 Effect of chloride on spectrum properties of Pr³⁺/Ho³⁺ co-doped fluorozirconate glasses

Ya Zou, Yajie Wang, Shuai Han, Ying Du, Danping Chen, Qihong Yang

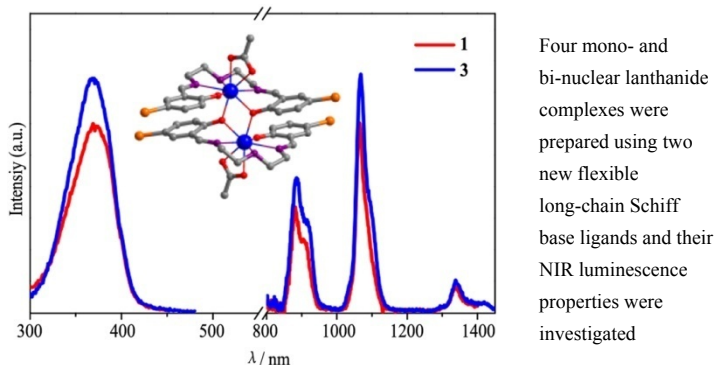


The luminescence intensity enhances with the increase of BaCl₂ concentration and then decreases gradually at higher BaCl₂ concentration. The luminescence intensity reaches the maximum and increases about three times when the BaCl₂ concentration is 7.5 mol%

J. Rare Earths, (38) 2020: 139-142

- 143 Construction of NIR luminescent nanoscale lanthanide complexes with new flexible Schiff base ligands

Bichen Yuan, Junbin Tao, Fei Wang, Chaoqun Zhu, Min Li, Xiaoping Yang



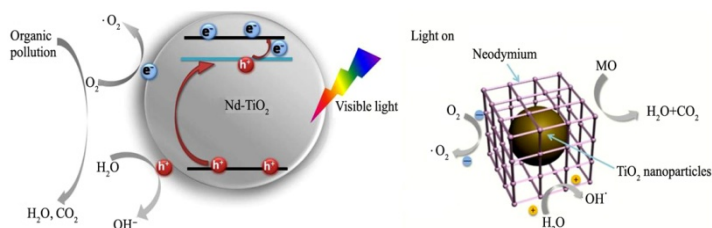
Four mono- and bi-nuclear lanthanide complexes were prepared using two new flexible long-chain Schiff base ligands and their NIR luminescence properties were investigated

J. Rare Earths, (38) 2020: 143-147

RARE EARTH CATALYSIS

- 148 Enhanced photocatalytic activities of Nd-doped TiO₂ under visible light using a facile sol-gel method

Jicai Liang, Jingya Wang, Kexian Song, Xiaofeng Wang, Kaifeng Yu, Ce Liang

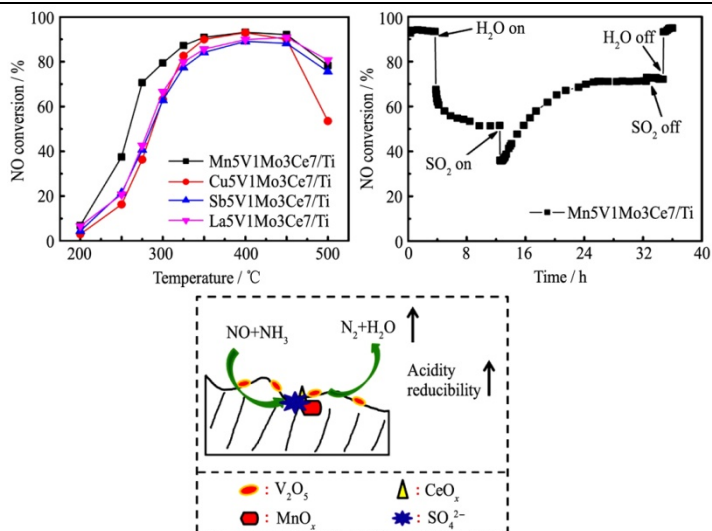


Titanium dioxide nanoparticles modified with neodymium were prepared with template-free sol-gel method. The photocatalytic activity of the obtained samples was evaluated by photodegradation of methyl orange in aqueous solution under ultraviolet-visible and visible irradiation. The experimental results show that the 1 mol% Nd-doped TiO₂ exhibits the highest degradation of 96.5% under visible irradiation. The modification has made an obvious promotion of photocatalyst activity

J. Rare Earths, (38) 2020: 148-156

- 157 Effects of MO_x (M=Mn, Cu, Sb, La) on V–Mo–Ce/Ti selective catalytic reduction catalysts

Daojun Zhang, Ziran Ma, Baodong Wang, Qi Sun, Wenqiang Xu, Tao Zhu

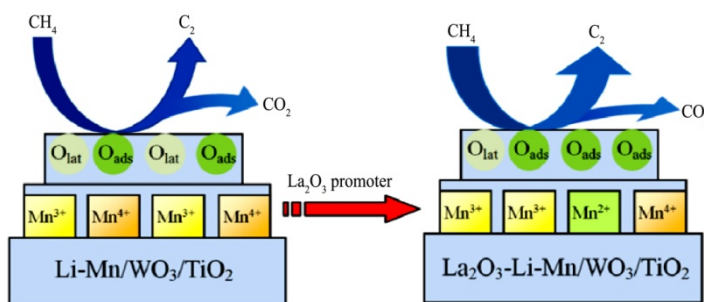


Mn5V1Mo3Ce7/Ti exhibits the best SCR performance. The acidity and reducibility of V1Mo3Ce7/Ti are enhanced by the addition of Mn. The sulphate species formed in the presence of SO₂ significantly enhance the H₂O and SO₂ tolerance of Mn5V1Mo3Ce7/Ti

J. Rare Earths, (38) 2020: 157-166

- 167 Enhancement of La_2O_3 to $\text{Li-Mn}/\text{WO}_3/\text{TiO}_2$ for oxidative coupling of methane

Fei Cheng, Jian Yang, Liang Yan, Jun Zhao, Huahua Zhao, Huanling Song, Ling Jun Chou

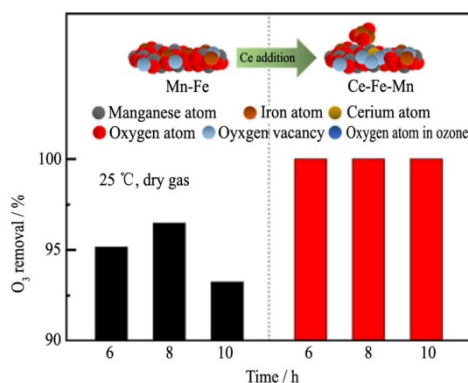


The incorporation of La_2O_3 alters the Mn valence state and oxygen property of the catalysts, which control the reaction performance

J. Rare Earths, (38) 2020: 167-174

- 175 Ce-Fe-Mn ternary mixed-oxide catalysts for catalytic decomposition of ozone at ambient temperatures

Xiao Chen, Zhenglong Zhao, Shuo Liu, Jinxing Huang, Jing Xie, Ying Zhou, Zhiyan Pan, Hanfeng Lu



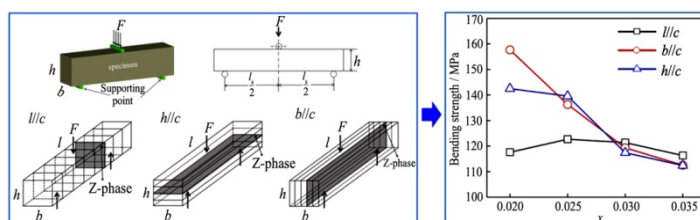
The Ce-Fe-Mn ternary mixed oxide catalyst displays better catalytic activity for O_3 decomposition than Mn-Fe binary mixed oxide catalyst. This superior activity that can be ascribed to the addition of a small amount of Ce into Mn-Fe mixed oxides causes lattice distortion. Fe separated out to form Fe_2O_3 , and the defects increased, forming more oxygen vacancies

J. Rare Earths, (38) 2020: 175-181

MAGNETISM AND MAGNETIC MATERIALS

- 182 Zirconium content induced mitigation of mechanical anisotropy in 2:17 type SmCo magnets

Guanghui Yan, Zhuang Liu, Yanping Feng, Weixing Xia, Chaoyue Zhang, Guangqing Wang, Aru Yan

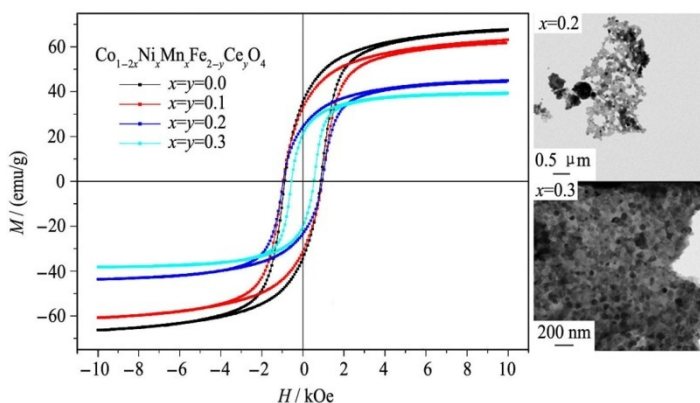


With increasing content of Zr in $\text{Sm}(\text{Co}_{0.91}\text{Fe}_{0.09}\text{Cu}_{0.09}\text{Zr}_x)_{7.68}$ magnets, the mechanical anisotropy is reduced. The increasing density of Z-phase induced by Zr content could make the decrease of bending strength in the case of loading F parallel to the c -axis of the magnets. The bending strength of the magnets with high Zr content under loading F perpendicular to the c -axis seems to be slightly higher than other two cases, which might be related to atom substitutions and crystal lattice distortion

J. Rare Earths, (38) 2020: 182-187

- 188 Synthesis and characterization of $\text{Co}_{1-2x}\text{Ni}_x\text{Mn}_x\text{Fe}_{2-y}\text{Ce}_y\text{O}_4$ nanoparticles

Munirah Abdullah Almessiere, Yassine Slimani, Abdulhadi Baykal



$\text{Co}_{1-2x}\text{Ni}_x\text{Mn}_x\text{Fe}_{2-y}\text{Ce}_y\text{O}_4$ ($0 \leq x=y \leq 0.3$) nanoparticles were successfully prepared by sol-gel auto-combustion method. All prepared samples exhibit soft ferromagnetic behavior

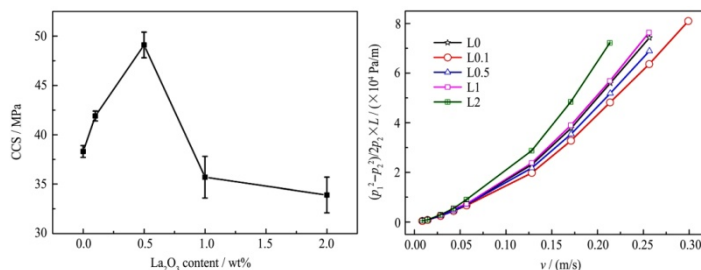
J. Rare Earths, (38) 2020: 188-194

ADVANCED RARE EARTH MATERIALS

- 195 Enhancing mechanical properties and air permeability of corundum porous materials by *in situ* formation of $\text{LaAl}_{11}\text{O}_{18}$ in bonding phase

Xin Xiong, Zhoufu Wang, Xitang Wang,
Hao Liu, Yan Ma

J. Rare Earths, (38) 2020: 195-202



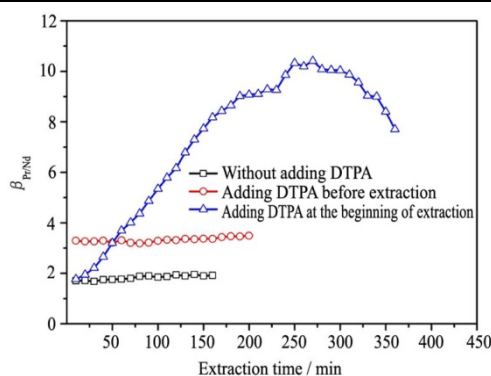
In this work, effects of *in situ* formed $\text{LaAl}_{11}\text{O}_{18}$ on the mechanical property and air permeability of corundum porous materials of particle-packing type were investigated. With a certain amount of La_2O_3 added, CCS and air permeability of the porous materials can be enhanced

CHEMISTRY AND HYDROMETALLURGY

- 203 Enhanced separation of praseodymium and neodymium by kinetic “push and pull” system of $[\text{A336}][\text{NO}_3]$ -DTPA in a column extractor

Xiaoqin Wang, Kun Huang, Wenjuan Cao,
Pan Sun, Na Sui, Weiyuan Song, Huizhou Liu

J. Rare Earths, (38) 2020: 203-212



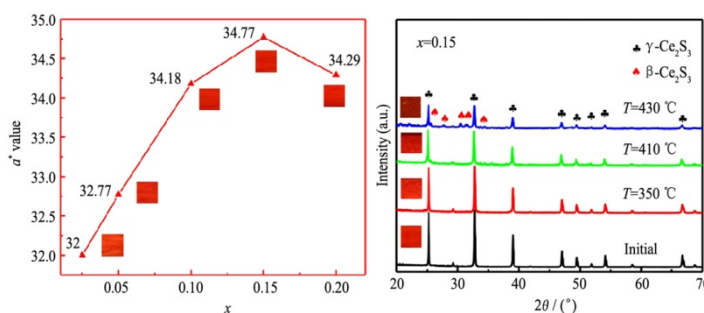
The separation between praseodymium and neodymium can be improved due to the kinetic “push and pull” effect from the rate order of Pr(III) and Nd(III) ions forming water-soluble complexes with DTPA in aqueous solutions being opposite to that of their extraction by $[\text{A336}][\text{NO}_3]$ oil droplets in column extractor

RARE EARTH APPLICATIONS

- 213 Effect of Sr^{2+} and Dy^{3+} co-doping on coloration and temperature stabilization of a $\gamma\text{-Ce}_2\text{S}_3$ red pigment

Yueming Li, Qi Liu, Fusheng Song,
Zhumei Wang, Zongyang Shen, Yan Hong

J. Rare Earths, (38) 2020: 213-218



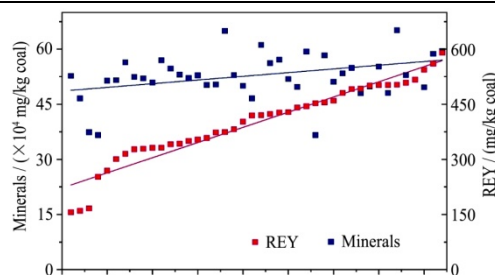
A series of environment-friendly red pigments Sr^{2+} and Dy^{3+} co-doped $\gamma\text{-Ce}_2\text{S}_3$ were synthesized at 730°C . The best red-color quality ($L^*=37.13$, $a^*=34.77$, $b^*=29.44$) is achieved when the pigment has a $\text{Dy}^{3+}/\text{Ce}^{3+}$ molar ratio of 0.15, and the material maintains its excellent red color ($L^*=31.49$, $a^*=30.94$, $b^*=25.33$) after being heated at 410°C for 30 min

GEOLOGY AND ORE DRESSING

- 219 Rare earth elements of fly ash from Wyoming's Powder River Basin coal

Zaixing Huang, Maohong Fan, Hanjing Tian

J. Rare Earths, (38) 2020: 219-226



The concentrations of rare earth elements derived from Powder River Basin coal are found to be scattered. However, the analysis shows that the rare earth element concentration is positively correlated to the mineral concentration, suggesting that the form of minerals might have impacts on the enrichment/detainment of rare earth elements which implies an alternative way of rare earth element beneficiation from coal fly ash